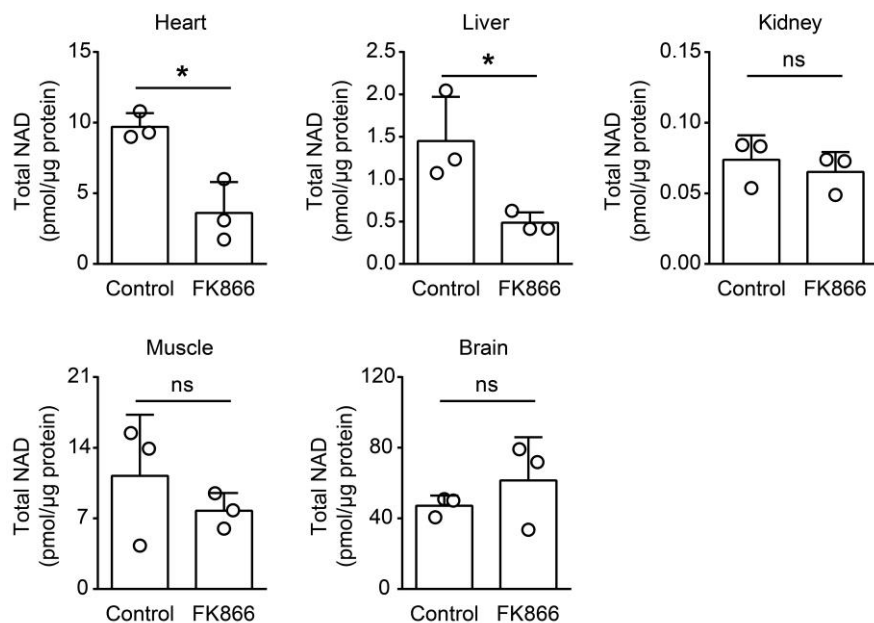


1  
2  
3  
4  
5  
6  
7  
8  
9

**Figure S1 NAMPT level changes in the mouse lungs during BLM-induced pulmonary fibrosis.**

(A) Representative graphs of HE, Masson's trichrome staining, and immunohistochemical staining of NAMPT in mouse lungs. Bar = 100  $\mu$ m. (B) Western blotting analysis and quantification for the expression of NAMPT in the lungs of mice. (C) ELISA analysis of extracellular NAMPT in BALF. Mean  $\pm$  SD (n = 3), \* $P$  < 0.05, \*\* $P$  < 0.01, \*\*\*\* $P$  < 0.0001, compared with Sham, unpaired  $t$ -test.



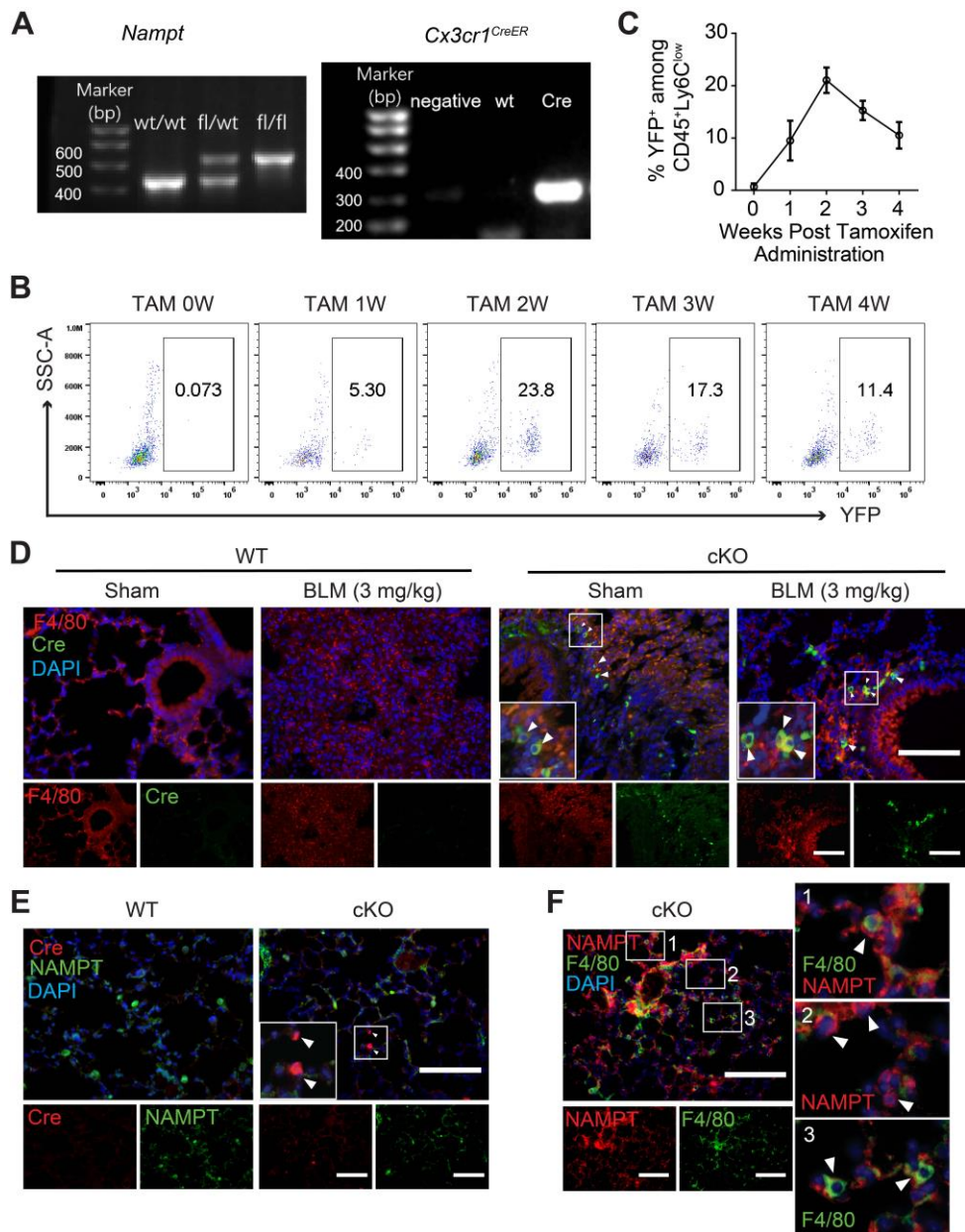
10

11

12 **Figure S2 Effect of FK866 on the NAD level in mouse tissues.**

13 Saline (Control) or 10 mg/kg FK866 (FK866) was administered once per day via intraperitoneal  
 14 injection for 16 consecutive days. After saline rinsing, mouse tissues (heart, liver, kidney, muscle,  
 15 and brain) were harvested, homogenized, and subjected to NAD determination using a commercial  
 16 kit. Mean ± SD (n = 3). \* $P < 0.05$ , unpaired  $t$ -test.

17

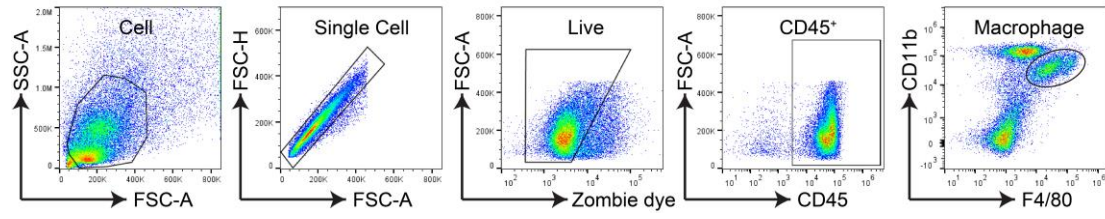


18

19

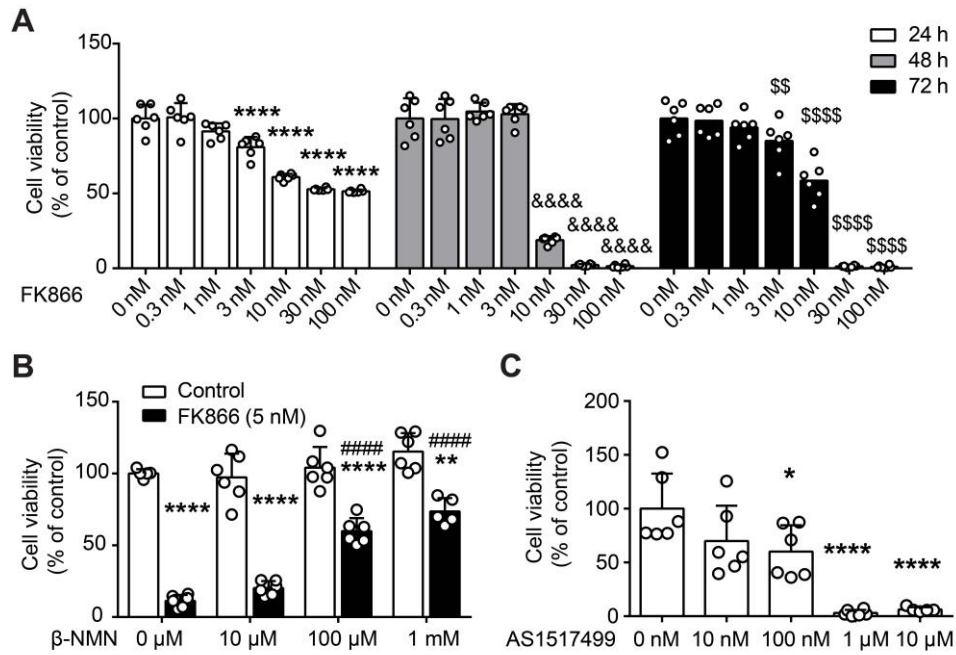
20 **Figure S3 Verification of specific knockout of NAMPT in monocytes/macrophages.**

21 (A) Gene identification of transgenic mice. (B, C) Time course of Cre expression after tamoxifen  
 22 administration by detecting the expression of the YFP reporter in peripheral blood monocytes  
 23 (CD45<sup>+</sup>Ly6C<sup>low</sup>). Mean ± SD (n = 3 mice per timepoint). (D) Immunofluorescence staining of  
 24 macrophage marker F4/80 (red) and Cre (green) in the lungs from control and NAMPT cKO mice.  
 25 (E) Immunofluorescence staining of Cre (red) and NAMPT (green) in the lung sections. (F)  
 26 Immunofluorescence staining of NAMPT (red) and F4/80 (green) in the lung of cKO mice. Bar =  
 27 100 μm (n = 3).



28  
29  
30  
31  
32

**Figure S4 Sequential gating strategy to identify lung macrophage subsets by flow cytometry analysis.**



33

34

35 **Figure S5 Effects of FK866, β-NMN, AS1517499 on the viability in RAW264.7 cells.**

36 RAW264.7 cells were treated with FK866 for 24 h, 48 h, 72 h or β-NMN, AS1517499 for 24 h,

37 and then CCK8 was added. The OD<sub>450</sub> was detected 2 h later. Mean ± SD (n = 6). \*\*\*\**P* < 0.0001,

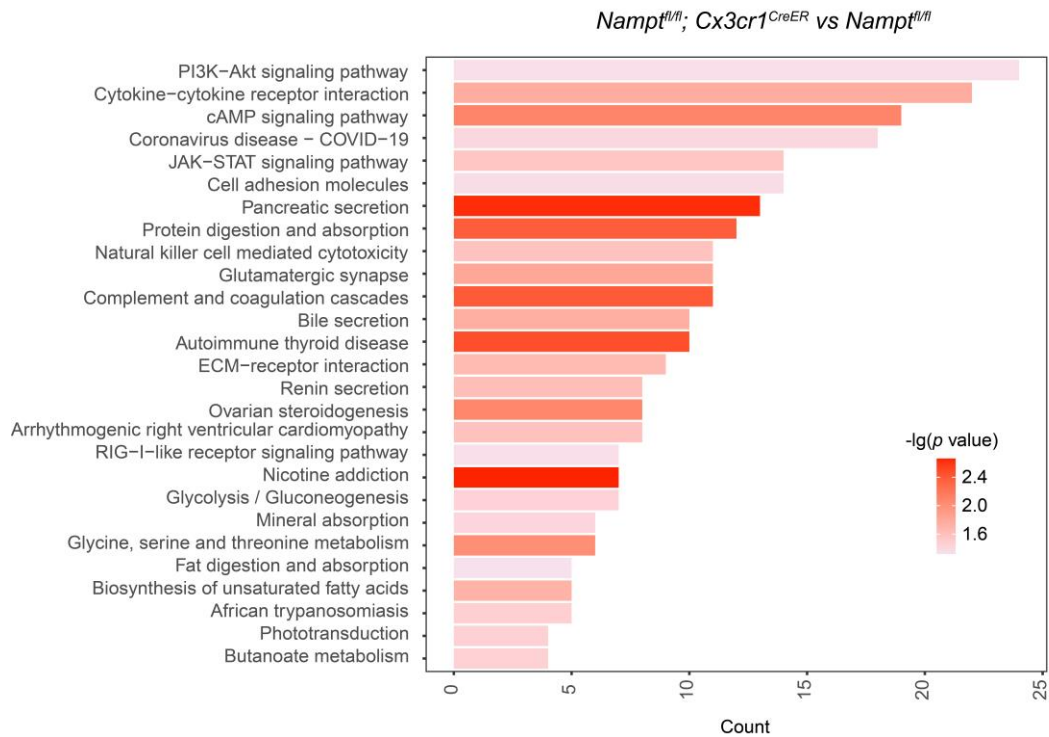
38 compared with 24 h-0 nM FK866; &&&&*P* < 0.0001, compared with 48 h-0 nM FK866; \$\$*P* < 0.01,

39 \$\$\$\$*P* < 0.0001, compared with 72 h-0 nM FK866 (A); \*\**P* < 0.01, \*\*\*\**P* < 0.0001, compared

40 with Control + 0 μM β-NMN; ####*P* < 0.0001, compared with FK866 + 0 μM β-NMN (B); \**P* <

41 0.05, \*\*\*\**P* < 0.0001, compared with 0 nM AS1517499 (C); one-way ANOVA.

42



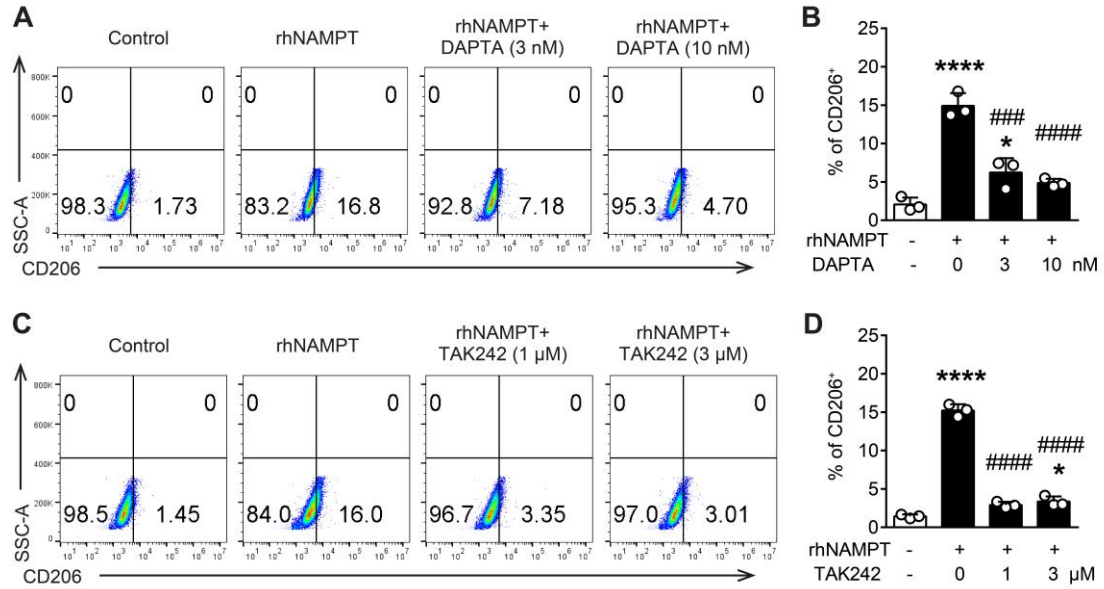
43

44

45 **Figure S6 A KEGG enrichment analysis of differentially expressed genes between**  
 46 **monocyte/macrophage NAMPT-specific deletion mouse (*Nampt<sup>fl/fl</sup>; Cx3cr1<sup>CreER</sup>*) and wild type**  
 47 **mouse (*Nampt<sup>fl/fl</sup>*).**

48 The vertical axis represents the cell signaling pathway category, and the horizontal axis represents  
 49 the enriched gene count. The color key represents the negative of log 10 (*p* value).

50



51

52

53 **Figure S7 Extracellular NAMPT-induced M2 polarization may be mediated by CCR5 and**  
 54 **TLR4.**

55 RAW264.7 cells were treated with CCR5 blocker DAPTA or TLR4 blocker TAK242 for 1 h, and  
 56 then rhNAMPT (300 nM) was added. The CD206<sup>+</sup> cells were detected using flow cytometry.

57 Mean ± SD (n = 3). \**P* < 0.05, \*\*\*\**P* < 0.0001, compared with Control; ###*P* < 0.001, ####*P* <

58 0.0001, compared with rhNAMPT, one-way ANOVA.